SUBBAND ADAPTIVE ARRAY FOR DS-CDMA MOBILE RADIO

Xuan Nam Tran, Takanori Omata*, Tetsuki Taniguchi and Yoshio Karasawa

Department of Electronic Engineering,
The University of Electro-Communications, Tokyo 182-8585, Japan
E-mail: namtx@radio3.ee.uec.ac.jp

1 Introduction

Digital mobile communications are affected by multipath fading and interference leading to reduced channel capacity and impaired signal quality. One of the approaches to overcome the problems is to use the spread spectrum or, specifically, direct sequence Code Division Multiple Access (DS-CDMA). The use of orthogonal codes with large processing gain in DS-CDMA can help to reduce the co-channel interference (CCI) and prevent users from interfering with each other, *i.e.*, reduce the multiple access interference (MAI). The effect of multipath fading causing interpath interference similar to inter-symbol interference (ISI) in Time Division Multiple Access (TDMA) systems can be mitigated by employing the RAKE receiver. Another approach to cancelling interference and increasing channel capacity is to employ array antenna at the base-station. The combination of array antenna and CDMA to maximise performance benefits was first presented by Compton in [1] and studied further in [2]-[7]. It has been clearly shown that this combination helps to greatly increase the channel capacity and reduce interference.

In this paper, we propose a novel scheme of adaptive array for DS-CDMA using subband adaptive signal processing. The scheme exploits the spreading code and pilot signal as the reference signal to estimate the propagation channel. By using subband signal processing, a large amount of computational load is saved. Moreover, as the correlation between multipaths is increased, the scheme can effectively combine multipaths to maximise the output SINR. Compared with 2D RAKE receivers proposed so far [5]-[7] the scheme provides relatively equivalent performance while having less computational load due to utilising adaptive signal processing in subbands. For this reason, the scheme is called *the implicit 2D RAKE receiver*. The configuration of the proposed novel scheme is shown in Fig. 1

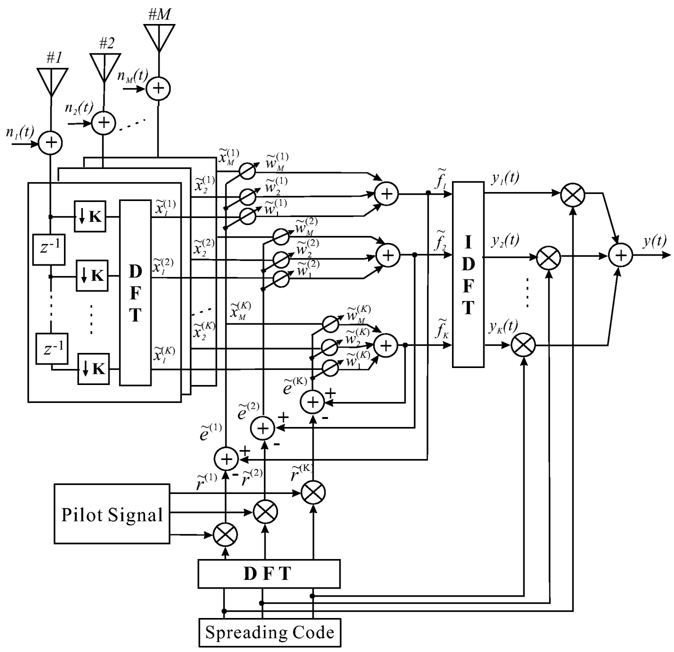

Figure 1: Subband adaptive array for DS-CDMA.

*The author is currently with J-Phone Communications Co., Ltd., Japan.

2 Configuration Description

Consider an asynchronous direct sequence spread BPSK system where after demodulation to remove the carrier frequency, the received signal of the i-th user is given by $s_i(t) = \alpha_i c_i(t) b_i(t)$, where α_i is the complex amplitude of the received signal, $b_i(t)$ is the i-th user's symbol and given by $b_i(t) = b_u \in \{-1, 1\}$ for BPSK modulation, $uT_b \le t < (u+1)T_b$, and $c_i(t)$ is the spreading code assigned to the i-th user with $c_i(t) = c_v \in \{-1, 1\}$, $vT_c \le t < (v+1)T_c$; T_b and T_c are the bit and chip intervals, respectively, and $P_G = T_b/T_c \gg 1$ is the processing gain.

Assume that the system is affected by multipath fading where the i-th user receives P_i multipaths with different amplitudes $\alpha_{i,p}$, delays $\tau_{i,p}$ and arrival angles $\theta_{i,p}$. Taking into consideration the effect of all the I users and noise, the received signal at the array can be written as

$$\boldsymbol{x}(t) = \sum_{i=0}^{I-1} \sum_{p=0}^{P_i-1} \alpha_{i,p} b_i(t - \tau_{i,p}) c_i(t - \tau_{i,p}) \boldsymbol{a}(\theta_{i,p}) + \boldsymbol{n}(t) \tag{1}$$

where $\boldsymbol{a}(\theta_{i,p}) = \begin{bmatrix} 1 & e^{-j\frac{2\pi d}{\lambda}\sin\theta_{i,p}} & \dots & e^{-j\frac{2(M-1)\pi d}{\lambda}\sin\theta_{i,p}} \end{bmatrix}^{\mathrm{T}}$ is the array steering vector corresponding to the p-th path of the i-th user's signal, $\boldsymbol{n}(t) = [n_1(t) \quad n_2(t) \quad \dots \quad n_M(t)]^{\mathrm{T}}$ is the noise vector containing independent and identically distributed (i.i.d) noise in each element, and $[.]^{\mathrm{T}}$ denotes the vector transpose operation. Now if we define $\boldsymbol{s}_{i,p}(t) = \alpha_{i,p} b_k(t - \tau_{i,p}) c_k(t - \tau_{i,p}) \boldsymbol{a}(\theta_{i,p})$ as the signal vector at the array from the p-th path of the i-th user, then (1) can be rewritten as

$$\boldsymbol{x}(t) = \sum_{i=0}^{I-1} \sum_{p=0}^{P_i-1} \boldsymbol{s}_{i,p}(t) + \boldsymbol{n}(t) \tag{2}$$

Next, the received signal $\boldsymbol{x}(t)$ is decimated with decimation rate D before being converted into frequency domain subbands. In our approach we use critical sampling, *i.e.*, the decimation rate D is equal to the number of subbands K. Since critical sampling is used, the analysis filter works as a serial-to-parallel (S/P) converter and converts serial signal samples into parallel subband samples. These subband samples in time domain are then transformed using the Discrete Fourier Transform (DFT) to give the subband signal vectors at n-th subband in frequency domain as[8]

$$\widetilde{\boldsymbol{x}}^{(n)} = \sum_{i=0}^{I-1} \sum_{p=0}^{P_i-1} \widetilde{\boldsymbol{s}}_{i,p}^{(n)} + \widetilde{\boldsymbol{n}}^{(n)} \tag{3}$$

In order to perform the adaptive signal processing in subbands, it is necessary that the reference signal also be converted into frequency domain subbands. In our proposed configuration, the reference signal is generated from the desired user spreading code and the pilot signal. First, the user spreading code is transformed into frequency domain using the DFT transform, and then this frequency domain spreading code is used to spread the pilot signal. Suppose that the 0-th user is taken as the desired user, the frequency domain reference samples at the n-th subband are given by $\widetilde{r}^{(n)} = \sum_{k=1}^{K} c_0(t - [k-1]T_c) b_0(t) e^{-j\frac{2\pi}{K}(n-1)(k-1)}$. In the training process the complex weights in subbands are updated by the error signal defined as the difference between the combined subband signal $\widetilde{f}^{(n)}$ and the reference signal in subbands $\widetilde{r}^{(n)}$ as $\widetilde{e}^{(n)} = \widetilde{f}^{(n)} - \widetilde{r}^{(n)}$. Using the mean square error $\mathrm{E}\big[\big\{\widetilde{e}^{(n)}\big\}^2\big]$ as a criterion to optimise the complex weights will result in the optimal weight vectors in subbands given by the well-known Wiener-Hopf equation

$$\boldsymbol{w}^{(n)} = (\boldsymbol{R}^{(n)})^{-1} \boldsymbol{p}^{(n)}, \tag{4}$$

where $\boldsymbol{R}^{(n)} = \mathrm{E}\big[\widetilde{\boldsymbol{x}}^{(n)} \big(\widetilde{\boldsymbol{x}}^{(n)}\big)^{\mathrm{H}}\big]$ are the covariance matrices and $\boldsymbol{p}^{(n)} = \mathrm{E}\big[\widetilde{\boldsymbol{x}}^{(n)} \big(\widetilde{r}^{(n)}\big)^{*}\big]$ are the reference correlation vectors in subbands. Here $\mathrm{E}[.]$, $(.)^{*}$ and $(.)^{\mathrm{H}}$ denote the expectation, the complex conjugate and the Hermitian operation, respectively.

The subband signals after be weighted by the optimal weights are combined according to each subband and the Inverse Discrete Fourier Transform (IDFT) is then performed on the combined signals $\widetilde{f}^{(n)}$ to give the array outputs $y_k(t)$ in time domain. To convert these array outputs in parallel into the serial signal a synthesis filter or a parallel-to-serial (P/S) converter for the case of the critical sampling SBAA is often needed [8]. However, in our approach instead of converting $y_k(t)$ into serial signal $y(t)$ we despread them by the desired user spreading code $c_0(t)$, and thus the synthesis filter bank is saved.

By using the proposed configuration of SBAA for DS-CDMA, several advantages can be achieved including a 2D RAKE's function despite its configuration is far different from that of the conventional 2D RAKE receivers. For this reason, we call the proposed SBAA for DS-CDMA as *an implicit 2D RAKE receiver*.

3 Simulation Results

In this section, we provide the simulation results of the implicit 2D RAKE receiver. The simulation model contains $M = 8$ antennas, $K = 31$ subbands using direct sequence spread BPSK with processing gain $P_G = 31$. The transmit data contains 1000 BPSK symbols and the sample matrix inversion (SMI) algorithm is employed to calculate the optimal weight vectors in subbands. The input SNR is set to 0dB. The simulation results of the standard 2D RAKE [6] are also shown to compare the performance of the two 2D RAKE configurations.

Figures 3 to 5 show the multipath combining capability of the implicit 2D RAKE. In Fig. 3, we assume that there are two multipaths incident at the array, the direct ray with $\theta_{0,0}$=0^0 and delay $\tau_{0,0} = 0$, and the delayed ray with $\theta_{0,1} = 30^0$ and delay $\tau_{0,1}$ varying from 0 to 20 chips. It is noticed that the implicit 2D RAKE has capability to combine multipaths with small delays. Figure 4 shows the output SINRs as the angle of arrival (AOA) of the delayed ray $\theta_{0,1}$ varies. It is clear that when the delay of the delay small, namely, when $\tau_{0,1} = 1$ chip the performances of the implicit 2D RAKE and the standard 2D RAKE are almost the same. However, as the delay of the delayed ray increases, the performance of the implicit 2D RAKE becomes worse than that of the standard 2D RAKE. Fig. 5 is the performance comparison of the two 2D RAKEs when the number of antenna elements and input SNR are varied. In this case, we assume that the received signal contains 3 multipaths: $\theta_{0,0} = 0^0/\tau_{0,0} = 0$ chip, $\theta_{0,1} = 15^0/\tau_{0,1} = 1$ chip, and $\theta_{0,2} = -20^0/\tau_{0,2} = 2$ chips. The input SNR is in turn set as -10dB, 0dB and 10dB. It is apparent from Fig. 5 that the performances of the two 2D RAKEs are relatively equivalent, particularly, for low input SINRs.

We now compare the MAI cancelling capabilities of the implicit 2D RAKE and the standard 2D RAKE. The propagation model is set up with 1 desired user and 3 other undesired users with interference to noise ratio INR=0dB as MAI sources. For each user we assume that there are 1 direct ray and 2 delayed rays with AOAs and delays (in chips) as in Fig. 2. In this case, the standard 2D RAKE gives output SINR about 1.3430 dB better than the implicit 2D RAKE does. The normalised power pattern of the two 2D RAKEs are compared in Fig. 6.

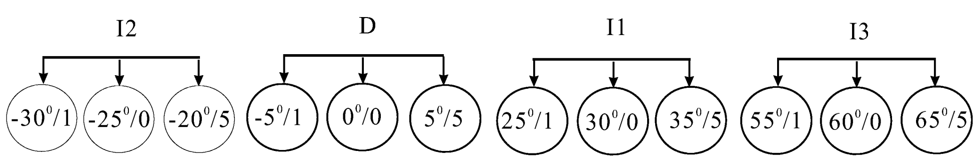

Figure 2: Propagation model with MAI interferences.

4 Conclusion

We have proposed a novel scheme of SBAA for DS-CDMA. It has been shown that the scheme has relatively equivalent performance with that of the standard 2D RAKE receiver, particularly, for low input SNRs.

References

[1] R.T. Compton, Jr., "An adaptive array in a spread-spectrum communications system," Proc. IEEE, vol. 66, pp. 289-298, Mar. 1978.

[2] R. Kohno, H. Imai, M. Hatori and S. Pasupathy, "Combination of an adaptive array antenna and a calceller of interference for direct-sequence spread-spectrum multiple-access system," vol. 8, no. 4, pp. 679-682, May 1990.

[3] H. Iwai, T. Shiokawa and Y. Karasawa, "An Investigation of Space-Path Hybrid Diversity Scheme for Base Station Reception in CDMA Mobile Radio," IEEE J. Selected Areas in Commun., vol. 12, no. 5, June 1994.

[4] A.J. Paulraj and C.B. Paradias, "Space-time processing for wireless communications," IEEE Signal Proc. Mag., vol. 14, no. 6, pp. 49-83, Nov. 1997.

[5] B. H Khalaj, A. Paulraj, and T. Kailath, "2D RAKE Receivers for CDMA Cellular Systems," in Proc. IEEE GLOBECOM '94, pp. 400-404, 1994.

[6] A. Stephene and B Champagne, "Improving the Performance of Blind CDMA 2D RAKE Receivers with Phase Ambiguity in the Bit Decision Variable," in Proc. 32th Asilomar Conf. Signals, Syst., Comput., pp. 1882-1886, California, USA, Nov. 1998

[7] T. Inoue and Y. Karasawa, "Two-Dimensional RAKE Reception Scheme for DS/CDMA Systems in Beam Space Digital Beam Forming Antenna Configuration," IEICE Trans. Commun. vol. E81-B, no. 7, July 1998.

[8] X. N. Tran, T. Taniguchi and Y. Karasawa, "Performance Analysis of Subband Adaptive Array in Multipath Fading Environment," IEICE Trans. Fund, Aug. 2002, (in press).

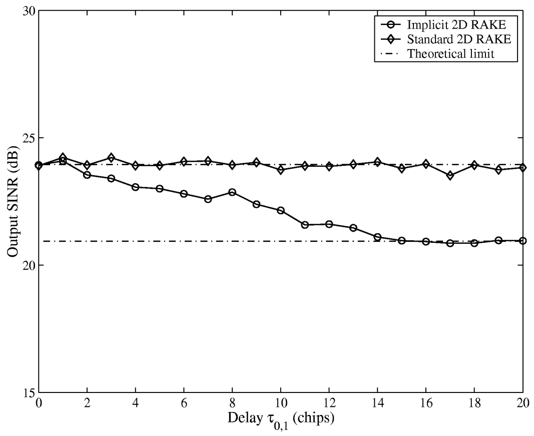

Figure 3: SINR versus delay of delayed path ($\theta_{0,0} = 0^0/\tau_{0,0} = 0$, $\theta_{0,1} = 30^0$)

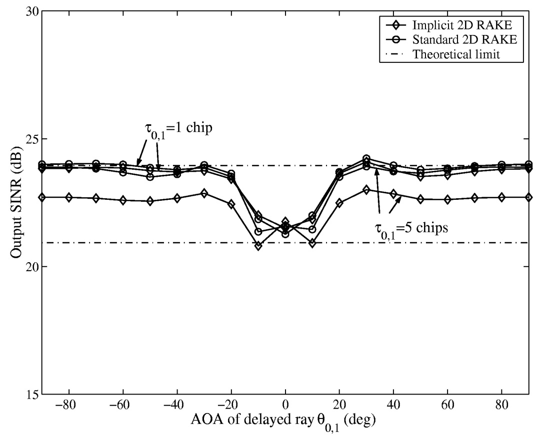

Figure 4: SINR versus AOA of delayed path ($\theta_{0,0} = 0^0/\tau_{0,0} = 0$, $\tau_{0,1} = 1$ and 5 chips)

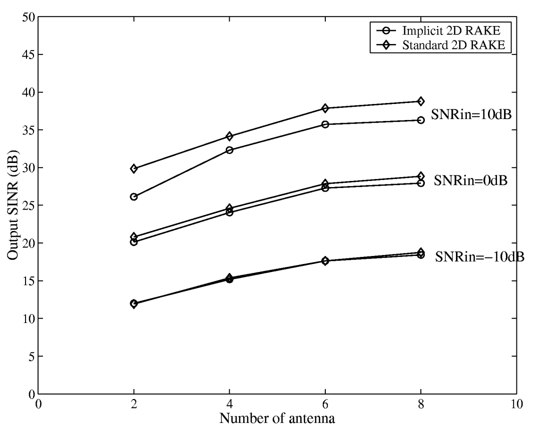

Figure 5: SINR versus number of antennas

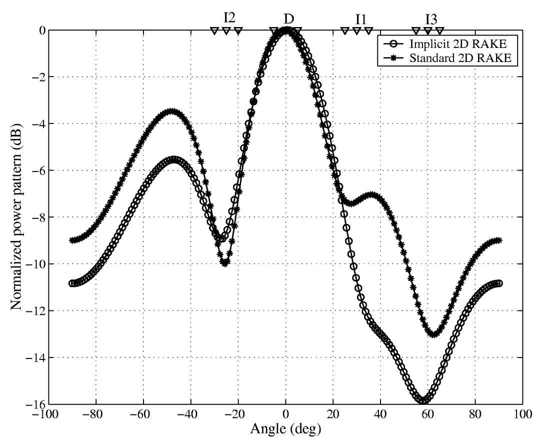

Figure 6: Normalised power patterns